

## Algebraic prediction of resonance couplings from assumptions about zero-trajectory slopes

G. v. Gehlen and W. Pfeil

*Physikalisches Institut, Universität Bonn, D-5300 Bonn, Germany*

(Received 10 October 1979)

The slopes of the amplitude zeros in the Mandelstam plane passing through the intersection of  $s$ -channel  $I = 3/2$  resonances with the  $u$ -channel nucleon pole are considered for pion-nucleon scattering, for pion production by vector and axial-vector currents, and for Compton scattering. New striking regularities relevant for the construction of explicit dual models involving fermions and currents are found. If one demands the zero slopes to be equal for all helicity amplitudes of the same process, the spin and parity structure of the resonance excitation is predicted in good agreement with experiment. Demanding the zeros to pass the intersection points close to the direction  $t \approx \text{constant}$ , the right order of magnitude of the resonance couplings is obtained.

### I. INTRODUCTION

More than ten years have passed since Veneziano<sup>1</sup> wrote down the first explicit dual resonance model (DRM). In the meantime there have been beautiful developments of this idea which lead close to a consistent formulation of dual multiparticle amplitudes and visualize these amplitudes in terms of the string picture.

Initially there was considerable excitement about possible phenomenological applications of DRM's: e.g., Lovelace<sup>2</sup> applied the four-point function to describe the Dalitz plot of  $\bar{p}n \rightarrow 3\pi$ ; then factorization from the five-point function provided further constraints for this process.<sup>3</sup> Peterson and Törnqvist<sup>4</sup> made encouraging applications of the five-point function to production processes like  $Kp \rightarrow \pi\pi\Lambda$ . Very important was also the discovery that the DRM, applied to inclusive reactions, automatically provides an exponential  $p_T$  cutoff.<sup>5</sup> However, very soon, serious problems became obvious when DRM was applied for such standard processes as pion-nucleon scattering<sup>6</sup> and pion photoproduction.<sup>7</sup> In these processes, e.g., parity doubling and fundamental problems with current amplitudes gave examples of the deficiencies of DRM's. At present, the field gets more and more abandoned, since the usefulness of DRM's for phenomenology seems to be rather limited.<sup>8</sup>

In the following, we want to point out some new regularities which perhaps may be helpful for more successful constructions of DRM amplitudes. Our approach follows the original line of Lovelace,<sup>2</sup> or, more specifically, the later work of Odorico: In his investigations, Odorico<sup>9</sup> put the emphasis on the study of the pattern of zero surfaces in the complex Mandelstam plane. If one has poles in different channels, e.g., a  $\Delta$  in the  $s$  channel and a nucleon pole in the  $u$  channel, quite generally, a zero is required to pass through the intersection point of these poles. A single Euler-

$B$ -function term gives such a zero in the direction of constant third Mandelstam variable (here  $t$ ), but, as has been stressed by Odorico, many other patterns of zeros are equally possible.

We concentrate on processes involving particles with spin and consider also current reactions, i.e., just those cases which in the past have encountered particular difficulties. These reactions are described by several independent helicity or spin amplitudes. We shall investigate the hypothesis that for a particular choice of basic amplitudes the double-pole-killing zeros have the same slope in all helicity amplitudes. In many cases we find that this leads to a successful non-trivial prediction of the spin pattern of the resonance excitation. Going further, and demanding the zeros to follow approximately, e.g.,  $t = \text{const}$ , we can accurately predict the absolute values of the resonance couplings. Although the latter procedure has been proposed before, e.g., in Ref. 9, we show that it is much more successful than previous authors believed. We stress that our aim is not so much to describe the data in all details, but rather to find out some main structure. Thus we are using the narrow-resonance approximation throughout. Nevertheless, in many cases our numerical results agree quite well with the experimental data.

Our approach, which is purely algebraical, has been stimulated by the regularities which we found in our phenomenological investigation of the zero structure of pion photoproduction.<sup>10</sup> However, since with broad resonances the zeros generally lie at complex values of  $s$  and/or  $t$ , a phenomenological determination of the zero surfaces requires an analytical continuation by means of a partial-wave analysis. Consequently it is strongly influenced by the still considerable uncertainties of such analyses.<sup>11</sup> Therefore we believe that our algebraic approach may be stimulating also for future phenomenological partial-wave analyses.

For pion-nucleon scattering very detailed phenomenological investigations of the zero surfaces have been performed by the Karlsruhe<sup>12</sup> and Berkeley groups.<sup>13</sup> A zero analysis is also available for pion-pion scattering.<sup>14</sup>

Our algebra will start from the following considerations which have been discussed in detail, e.g., by Odorico<sup>9</sup>: Consider an amplitude  $f$  which has an  $s$ -channel resonance at  $s = M^2 - i\Gamma M$  and a  $u$ -channel pole at  $u = m^2$  (compare Fig. 1). In the vicinity of the intersection point of the two poles we approximate

$$f(s, u) \approx \frac{r_s}{s - M^2 + iM\Gamma} + \frac{r_u}{u - m^2} \quad (1.1)$$

$$= \frac{(r_u - r_s)(s - M^2 + iM\Gamma) - r_s(t - t_i)}{(s - M^2 + iM\Gamma)(u - m^2)}, \quad (1.2)$$

where  $\Gamma$  is the total resonance width and

$$t_i = \sum m_i^2 - M^2 + iM\Gamma - m^2. \quad (1.3)$$

$\sum m_i^2$  is the sum of the external mass squares;  $r_s$  and  $r_u$  are the pole residua, evaluated at the intersection. From Eq. (1.2) we see that near  $t = t_i$ ,  $f$  has a zero trajectory satisfying

$$t - t_i = \left( \frac{r_u}{r_s} - 1 \right) (s - M^2 + iM\Gamma), \quad (1.4)$$

which has the slope

$$\xi \equiv \left. \frac{dt}{ds} \right|_{t=t_i} = \frac{r_u}{r_s} - 1. \quad (1.5)$$

Here we shall always assume the limit of narrow resonances.  $r_s$  is related to  $\text{Im}f(s = M^2, t)$ , which we shall abbreviate by  $\text{Im}f^R$ :

$$r_s = -M\Gamma \text{Im}f^R. \quad (1.6)$$

Equations (1.5) and (1.6) now give the relation between  $\xi$ ,  $\text{Im}f^R$ , and  $r_u$  which we shall study for a

number of particular reactions:

$$(1 + \xi)M\Gamma \text{Im}f^R = -r_u. \quad (1.7)$$

In the following,  $r_u$  will always be the explicitly known expression of the Born amplitude. Forming the ratios of different helicity amplitudes and assuming that their zero trajectories all have the same slope  $\xi$ , the ratios of the  $\text{Im}f^R$  are completely determined by the ratios of the  $r_u$  since the factors  $M\Gamma(1 + \xi)$  drop out.

As is well known, no convincing criteria are available which tell us which particular spin amplitudes should be used. Even demanding good analytic properties, various choices remain, e.g., relativistic amplitudes [ $A(s, t)$  and  $B(s, t)$  for  $\pi$ - $N$  scattering], or parity-conserving helicity amplitudes, etc. This is an important problem if one wants to study amplitude zeros, since in general, by forming linear combinations the zero structures get completely changed. However, by demanding that the zero-trajectory slopes  $\xi$  at the pole intersections should be the same in all spin amplitudes of the same process, we force the zeros to coincide at least near the pole intersections. So we minimize the ambiguity caused by the choice of a particular set of amplitudes.

In Sec. VI we explain why it is not reasonable to ask that also different isospin amplitudes should have the same zero-trajectory slopes. So the problem of the choice of a special set of isospin amplitudes remains. We shall give an argument that for  $I_s = \frac{3}{2}$  our results should not be strongly dependent on the particular choice of isospin amplitudes which have been made.

In Sec. II we study the consequences of our hypothesis for  $I_s = \frac{3}{2}$  pion-nucleon scattering, Sec. III gives the analogous application to pion photoproduction, and Sec. IV treats Compton scattering. The case of weak axial-vector-current pion production in Sec. V brings unpleasant problems. Section VI contains a discussion of the isospin problem. Finally, Sec. VII summarizes our conclusions.

## II. PION-NUCLEON ELASTIC SCATTERING

We choose to work with  $s$ -channel helicity amplitudes  $f_{\pm}$  which have the half-angle factors removed (see the definitions given in Appendix A). Consider now an  $s$ -channel resonance at  $s = M^2 - i\Gamma M$  with angular momentum  $j = l + \frac{1}{2}$  and parity  $(-1)^{l+1}$  [like the  $\Delta(1232)$ ]. Then, according to the partial-wave expansion of the  $f_{\pm}$ , Eq. (A3), we write the resonance contribution analogously to Eq. (1.6) as

$$f_{\pm} = - \frac{\Gamma M \text{Im}f_{\pm}^R}{s - M^2 + i\Gamma M} [P'_{l+1}(x) \mp P'_l(x)]. \quad (2.1)$$

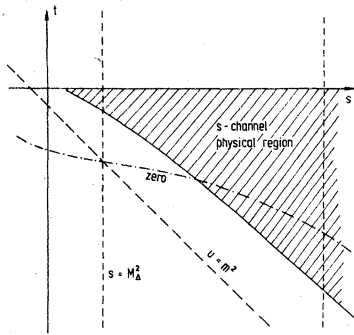


FIG. 1. The Mandelstam plane (e.g., here for pion photoproduction), showing the  $s$ -channel  $\Delta$  pole and the  $u$ -channel nucleon pole together with the zero trajectory passing through the pole intersection.

Here  $x$  is the cosine of the scattering angle and  $\text{Im}f_{i\pm}^R$  means  $\text{Im}f_{i\pm}$  evaluated at the resonance energy. In a narrow-resonance approximation, we thus get in the neighborhood of the intersection of  $s=M^2$  with  $u=m^2$  ( $m$  is the nucleon mass):

$$f_{\pm} = \frac{r_{\pm}^u}{u-m^2} - \frac{\Gamma M \text{Im}f_{i\pm}^R}{s-M^2} (P'_{i+1}(x_0) \mp P'_i(x_0)) + \dots \quad (2.2)$$

The nucleon-pole residues are given explicitly in Appendix A, Eqs. (A5);  $x_0$  is the unphysical value of  $x$  at the intersection, see Eq. (A6). Since we are considering an elastic process, we have

$$\Gamma \text{Im}f_{i\pm}^R = \Gamma_{e1} / |\vec{q}|, \quad (2.3)$$

where  $\Gamma_{e1}$  is the elastic width of the resonance. A formula very similar to Eq. (2.3) is obtained if the  $s$ -channel resonance instead has the parity  $(-1)^l$ : one has just to replace  $f_{i\pm}$  by  $\pm f_{i+1,-}$  according to Eq. (A3).

As has been shown in Eq. (1.7) of the Introduction, the ratios of the residues in Eq. (2.1) determine the zero-trajectory slopes in the amplitudes  $f_{\pm}$  at the intersection of the poles. Taking into account Eq. (2.3), we get from Eq. (2.2) if the  $s$ -channel resonance is in  $f_{i\pm}$  [i.e., its parity is  $(-1)^{l+1}$ ]

$$\Gamma_{e1} M(1 + \xi_{\pm}) = - \frac{|\vec{q}| r_{\pm}^u}{P'_{i+1}(x_0) \mp P'_i(x_0)}. \quad (2.4)$$

If the resonance is in  $f_{i+1,-}$ , there is just an additional  $\pm$  sign:

$$\Gamma_{e1} M(1 + \xi_{\pm}) = \mp \frac{|\vec{q}| r_{\pm}^u}{P'_{i+1}(x_0) \mp P'_i(x_0)}. \quad (2.5)$$

Let us now discuss these relations in turn for the  $\Delta(1232)$ , the  $F_{37}(1945)$ , and for the high- $s$  limit.

#### A. The $\Delta(1232)$ resonance

For the  $\Delta$  in the  $s$  channel we have

$$P'_{i+1}(x_0) \mp P'_i(x_0) = 3x_0 \mp 1, \quad (2.6)$$

where from Eq. (A6) we find numerically that  $x_0 = -4.77$ . Using Eqs. (A5) and (A6) we get, since  $\Gamma \approx \Gamma_{e1}$ :

$$\Gamma(1 + \xi_{\pm}) = \frac{g^2}{6\pi} \frac{\vec{q}^3}{M^2} \frac{Wq_0 - \mu^2}{Eq_0 - \mu^2/2 - \vec{q}^2/3} \quad (2.7)$$

and

$$\Gamma(1 + \xi_{\pm}) = \frac{g^2}{6\pi} \frac{\vec{q}^3}{M^2} \frac{mq_0}{Eq_0 - \mu^2/2 - \vec{q}^2/3}. \quad (2.8)$$

The right-hand sides of Eqs. (2.7) and (2.8) have the values 0.089 and 0.083 GeV, respectively. This shows that indeed we have  $\xi_{+} \approx \xi_{-}$ . More precisely, using  $\Gamma = 0.115$  GeV, we find

$$\xi_{+} = -0.23, \quad \xi_{-} = -0.28, \quad (2.9)$$

so that in both amplitudes the zero trajectories pass the intersection point nearly in the direction  $t = \text{const}$  as in a one-term Euler- $B$ -function model.

The old well-known Chew-Low static model<sup>15</sup> gave a quite similar formula for the width of the  $\Delta(1232)$ :

$$\Gamma_{\text{Chew-Low}}^{\Delta} = \frac{g^2}{6\pi} \frac{\vec{q}^3}{M^2} \frac{M(M+m)}{2m^2} = 0.115 \text{ GeV}. \quad (2.10)$$

Omitting in the denominator of Eq. (2.8) the small term  $-\mu^2/2 - \vec{q}^2/3 \approx -2\mu^2$ , one notices the similarity of both expressions. Remember that also in the Chew-Low model, the  $\Delta$  width is determined by the  $u$ -channel nucleon pole.

#### B. The $F_{37}(1945)$ resonance

According to Eq. (2.4) for the  $F_{37}$ /nucleon-pole intersection, approximately equal slopes  $\xi_{+} \approx \xi_{-}$  are obtained if

$$\frac{Wq_0 - \mu^2}{mq_0} \approx \frac{P'_4(x_0) - P'_3(x_0)}{P'_4(x_0) + P'_3(x_0)}. \quad (2.11)$$

Actually, for  $W = 1.945$  GeV the left- and right-hand sides of Eq. (2.11) are 2.05 and 1.82, respectively [shifting the energy  $W$  somewhat does not improve (2.11) much since both sides have a very similar  $W$  dependence].

Using  $\Gamma = 0.23$  GeV (Ref. 16) and inserting numerical values for the right-hand side of Eq. (2.4), we obtain

$$(1 + \xi_{-})\Gamma_{e1}/\Gamma = 0.39, \quad (2.12)$$

which for  $\xi_{-} \approx 0$  is in excellent agreement with  $\Gamma_{e1}/\Gamma \approx 0.40$  of Ref. 16.

#### C. High-energy limit

We finally go to high energies in the  $s$  channel and neglect  $m^2$  and  $\mu^2$  compared to  $s$ . Then  $x_0$ , the  $s$ -channel scattering angle at the intersection point of a high-energy  $\Delta$  resonance with the nucleon pole, becomes approximately

$$x_0 \approx -1 - m^2/2\vec{q}^2. \quad (2.13)$$

For  $x_0$  close to  $-1$  and large  $l$  we approximate the  $P'_i(x_0)$  and  $P'_{i+1}(x_0)$  of Eqs. (2.4) and (2.5) in terms of modified Bessel functions  $I_0$  and  $I_1$  (see, e.g., Ref. 17):

$$P'_{i+1}(x_0) + P'_i(x_0) \approx (-1)^l (l+1) I_0(R), \quad (2.14)$$

$$P'_{i+1}(x_0) - P'_i(x_0) \approx (-1)^l (l+1)^2 2I_1(R)/R, \quad (2.15)$$

with

$$R = (l + \frac{1}{2}) [2(1 - |x_0|)]^{1/2} \approx (l + \frac{1}{2}) m / |\vec{q}|. \quad (2.16)$$

Since for high  $s$  we have

$$r_+^u/r_-^u \approx W/m, \quad W \approx 2|\vec{q}|, \quad (2.17)$$

from Eqs. (2.4) and (2.5) we get for parity  $\pm (-1)^{l+1}$  resonances with  $I_s = \frac{3}{2}$ ,

$$\frac{1 + \xi_+}{1 + \xi_-} \approx \pm \frac{I_0(R)}{I_1(R)}. \quad (2.18)$$

If, more specially, we consider peripheral resonances lying on a square-root trajectory<sup>18</sup>

$$l + \frac{1}{2} = |\vec{q}|a, \quad (2.19)$$

with the radius  $a$  fixed, say at  $a = 1.05$  fm, then  $R$  has the energy-independent value

$$R = ma = 5. \quad (2.20)$$

Even for  $R \approx 5$  the approximation (2.14), (2.15) is very good. In Eq. (2.18) we get

$$I_0(5)/I_1(5) = 1.12. \quad (2.21)$$

From Eqs. (2.18) and (2.21) we see that in the case of resonances in  $f_{l+}$ , the slopes  $\xi_+$  and  $\xi_-$  have to be almost equal. However, in contrast, for  $f_{l+,-}$  resonances,  $1 + \xi_+$  and  $1 + \xi_-$  must be of opposite sign. Thus demanding  $\xi_+ \approx \xi_-$  excludes such resonances. This agrees well with the fact that for  $I_s = \frac{3}{2}$  no dominant resonances with parity  $(-1)^l$  have been observed.

For  $s \gg m^2$  and large  $l$ , the relation between  $\Gamma_{el}$  and  $\xi_-$  provided by Eq. (2.4) reads

$$\Gamma_{el}(1 + \xi_-) = (-1)^{l+1} \frac{g^2}{8\pi I_0(R)} \frac{m}{l+1}. \quad (2.22)$$

Assuming  $\xi_- > -1$ , we see that Eq. (2.22) also excludes parity  $(-1)^{l+1}$  resonances for even  $l$ , again in agreement with phenomenology. Specializing to peripheral resonances according to Eqs. (2.19) and (2.20), Eq. (2.22) simplifies to

$$\Gamma_{el}(1 + \xi_-) = \frac{0.25 \text{ GeV}}{l + \frac{1}{2}}. \quad (2.23)$$

It is instructive to estimate the contribution  $\sigma_{\text{periph}}^{(3/2)}$  of these peripheral  $I = \frac{3}{2}$  resonances (with even parity and  $l$  odd) to the total cross section. Assuming a sequence of narrow resonances at  $W = M_l (l = 1, 3, 5, \dots)$ , one has generally:

$$\sigma_{\text{tot}} = \sum_l \frac{2\pi^2}{\vec{q}_l^2} (l+1) \Gamma_{el}^l \delta(W - M_l). \quad (2.24)$$

For our series of odd- $l$  peripheral resonances satisfying Eqs. (2.19) and (2.22) for high  $s$ , this leads to

$$\sigma_{\text{periph}}^{(3/2)} = \sum_{l=1,3,\dots} \frac{\pi g^2 m \delta(W - M_l)}{s I_0(R) (1 + \xi_-)} \quad (2.25)$$

$$= \frac{\pi g^2 R}{s I_0(R) (1 + \xi_-)}, \quad (2.26)$$

since  $2dl = a dW$ . If we assumed  $\xi_- = 0$ , we would get

$$\sigma_{\text{periph}}^{(3/2)} \approx 41 \text{ mb GeV}^2/s. \quad (2.27)$$

Considering that the  $\pi^+p$  total cross section falls by 7.5 mb going from  $s = 6$  to  $s = 200 \text{ GeV}^2$ ,<sup>19</sup> we see that Eq. (2.27) gives quite the right order of magnitude of the nondiffractive cross section. Of course, one expects a decrease rather like  $s^{-1/2}$ , which from Eq. (2.25) may be obtained by a variation of  $\xi_-$  with energy or by including also resonances which are not quite peripheral.

Resonances not fulfilling Eqs. (2.19) and (2.20) may be included simply by smearing of the values of  $a$ . Since the Bessel functions  $I_i(R)$  increase exponentially with  $R$ , ancestors with respect to the peripheral resonances quickly get a very narrow width and will contribute little to  $\sigma_{\text{tot}}^{(3/2)}$ .

From the success of the calculations presented in this section, we see that the problems which have been encountered in applying DRM's to pion-nucleon scattering (see, e.g., Ref. 6), must not be cured in a way which changes the zero structure, at least for the  $s$ -channel  $\Delta$  ( $u$ -channel  $N$ ) term. We have seen that from this zero-trajectory structure there follows a number of phenomenologically correct and nontrivial predictions.

### III. PION PHOTOPRODUCTION

The requirement that the zero trajectories cross the pole intersection with the same slope in all helicity amplitudes, obviously becomes more stringent if we consider reactions with a more complicated spin structure. So it is interesting to check whether it leads also to reasonable results in the case of pion photoproduction and Compton scattering, moreover since dual models have particular problems with current amplitudes.

For the treatment of pion photoproduction we use amplitudes  $\hat{H}_i$  which are the Walker helicity amplitudes<sup>20</sup> with the half-angle factors removed. In terms of Walker's partial waves  $A_{l\pm}, B_{l\pm}$  the  $\hat{H}_i$  have the partial-wave expansions<sup>20</sup>:

$$\hat{H}_{1,3} = \sum_l (B_{l+} \mp B_{l+1,-}) (P_l'' \mp P_{l+1}''), \quad (3.1)$$

$$\hat{H}_{2,4} = \sum_l (A_{l+} \mp A_{l+1,-}) (P_l' \mp P_{l+1}'). \quad (3.2)$$

The residues  $r_i^u$  of the  $u$ -channel nucleon pole in the amplitudes  $\hat{H}_i$  for  $I_s = \frac{3}{2}$  are given in Appendix B. The cosine of the  $s$ -channel angle at the intersection point of  $s = M^2$  with  $u = m^2$ , is now given by

$$x_0 = (q_0 - M)/|\vec{q}|. \quad (3.3)$$

In analogy to Eq. (2.1), we write the  $s$ -channel

resonance terms as

$$A_{l\pm}^{(3/2)} = \frac{-\Gamma M \text{Im} A_{\frac{3}{2}}^R}{s - M^2 + i\Gamma M} \quad (3.4)$$

(similarly for  $B_{l\pm}$ ). We shall first consider only  $l = \frac{3}{2}$  resonances with parity  $(-1)^{l+1}$  and their intersection with the nucleon pole in the  $u$  channel. This leads us to four equations of the type Eq. (1.7):

$$(1 + \xi_{1,3}) \text{Im} B_{l+}^R = \frac{-\gamma_{1,3}^u}{M\Gamma [P_l'(x_0) \mp P_{l+1}'(x_0)]}, \quad (3.5)$$

$$(1 + \xi_{2,4}) \text{Im} A_{l+}^R = \frac{-\gamma_{2,4}^u}{M\Gamma [P_l'(x_0) \mp P_{l+1}'(x_0)]}, \quad (3.6)$$

where the  $\xi_i$  are the zero-trajectory slopes in the amplitudes  $\hat{H}_i$  for  $I_s = \frac{3}{2}$ .

Now we consider again several special cases as we did before in Sec. II.

#### A. The $\Delta(1232)$ resonance

Using  $A_{1+} = \frac{1}{2}(M_{1+} + 3E_{1+})$  and  $B_{1+} = E_{1+} - M_{1+}$  and inserting numbers on the right-hand side of Eqs. (3.5) and (3.6) for  $l = 1$ , we get (for  $\Gamma = 0.115$  GeV)

$$(1 + \xi_{1,3}) \text{Im}(M_{1+}^R - E_{1+}^R) = \begin{cases} 18.0 \\ 20.8 \end{cases}, \quad (3.7)$$

$$(1 + \xi_{2,4}) \text{Im}(M_{1+}^R + 3E_{1+}^R) = \begin{cases} 16.5 \\ 22.1 \end{cases}, \quad (3.8)$$

where  $\text{Im} M_{1+}^R$  and  $\text{Im} E_{1+}^R$  are defined in analogy to Eq. (3.4) and the unit is  $10^{-2}$  GeV $^{-1}$ .<sup>21</sup> The numbers in Eqs. (3.7) and (3.8) tell us

(i) Without further assumptions,  $\xi_1$  and  $\xi_3$  must be nearly equal, similarly  $\xi_2$  and  $\xi_4$ .

(ii) If we demand all four slopes  $\xi_i$  to be approximately equal, we get

$$M_{1+}^R \gg E_{1+}^R, \quad (3.9)$$

which is the well known selection rule, e.g., of the quark model.

(iii) Using from multipole analyses<sup>11</sup>  $\text{Im} M_{1+}^R = 0.27$  GeV $^{-1}$  and  $\text{Im} E_{1+}^R \ll \text{Im} M_{1+}^R$ , then in our crude narrow resonance approximation we obtain, e.g.,  $\xi_3 = -0.23$ . This is very similar to the small slope found in Eq. (2.9) for pion-nucleon scattering. So the zero trajectories in all four  $\hat{H}_i$  pass the  $s = M_\Delta^2/u = m^2$  crossing point nearly in the direction  $t = \text{const}$ . Of course, this argument may be turned around: Assuming the  $\xi_i \approx 0$ , we predict the value  $\text{Im} M_{1+}^R \approx 0.2$  GeV $^{-1}$ . This is 30% low, but not bad if we remember the simplifying narrow-resonance approximation.

#### B. The $F_{37}(1945)$ resonance

The same procedure for the  $F_{37}(1945)$  gives, using  $\Gamma = 0.23$  GeV (our unit is again  $10^{-2}$  GeV $^{-1}$ )

$$(1 + \xi_{1,3}) \text{Im}(M_{3+}^R - E_{3+}^R) = \begin{cases} 1.03 \\ 1.12 \end{cases}, \quad (3.10)$$

$$(1 + \xi_{2,4}) \text{Im}(M_{3+}^R + \frac{5}{3}E_{3+}^R) = \begin{cases} 0.84 \\ 1.15 \end{cases}. \quad (3.11)$$

Again we see that we must have  $\xi_1 \approx \xi_3$  and  $\xi_2 \approx \xi_4$ . Assuming  $\xi_{1,3} \approx \xi_{2,4}$ , it follows that  $E_{3+}^R \ll M_{3+}^R$ , as predicted in the quark model. Finally,  $\xi_i \approx 0$  leads to the prediction  $\text{Im} M_{3+}^R = 1.0 \times 10^{-2}$  GeV $^{-1}$ , which is consistent with the value

$$\text{Im} M_{3+}^{(3/2)R} = 1.15 \times 10^{-2} \text{ GeV}^{-1}, \quad (3.12)$$

given by multipole analyses of the experimental data.<sup>11</sup>

#### C. High-energy limit

Also the high-energy limit (always for  $I_s = \frac{3}{2}$ ) leads to an interesting result: We take  $s \gg m^2, \mu^2$  and use the simplified expressions of the  $\gamma_i^u$  given in Appendix B, Eqs. (B10)–(B13). Equation (3.3) becomes

$$x_0 \approx -1 - m^2/(2\bar{q}^2). \quad (3.13)$$

We approximate the spherical harmonics by Eqs. (2.14) and (2.15) and use

$$P_{l+1}''(x_0) + P_l''(x_0) \approx (-1)^{l+1} l(l+1)(l+2)I_1(R)/R, \quad (3.14)$$

$$P_{l+1}''(x_0) - P_l''(x_0) \approx (-1)^{l+1} l(l+2)(l+1)^2 2I_2(R)/R^2, \quad (3.15)$$

with  $I_1$  and  $I_2$  denoting spherical Bessel functions.  $R$  is defined in Eq. (2.16). The generalization of Eq. (3.7), etc., is now, inserting Eqs. (B10)–(B13) and assuming  $l \gg 1$ :

$$-\frac{1}{2}l \text{Im} B_{l+}^R (1 + \xi_{1,3}) = \tilde{\gamma}(\kappa \mp 1)/I_{2,1}(R), \quad (3.16)$$

$$\text{Im} A_{l+}^R (1 + \xi_{2,4}) = \tilde{\gamma}(\kappa \mp 1)/I_{1,0}(R), \quad (3.17)$$

with

$$\kappa = 1 + g_V = 4.706, \quad (3.18)$$

and

$$\tilde{\gamma} = \frac{egm}{16\pi|\bar{q}|a\Gamma M}. \quad (3.19)$$

We conclude as follows.

(i) One obtains  $\xi_1 = \xi_3$  if

$$\frac{\kappa - 1}{\kappa + 1} = \frac{I_2(R)}{I_1(R)}, \quad (3.20)$$

and  $\xi_2 = \xi_4$  if

$$\frac{\kappa - 1}{\kappa + 1} = \frac{I_1(R)}{I_0(R)}. \quad (3.21)$$

For peripheral resonances fulfilling Eqs. (2.19)

and (2.20) the right-hand sides of Eqs. (3.20) and (3.21) have the values 0.72 and 0.89, respectively. Comparing this to  $(\kappa - 1)/(\kappa + 1) = 0.65$  we see that  $\xi_1 \approx \xi_3$  and  $\xi_2 \approx \xi_4$  is crudely satisfied.

(ii) Requiring  $\xi_3 \approx \xi_4$  leads to

$$-\frac{1}{2}l \text{Im}B_{i_+}^R \approx (\text{Im}A_{i_+}^R)I_1(R)/I_0(R). \quad (3.22)$$

This means that, in order to have all four slopes  $\xi_i$  approximately equal, we must have *nearly pure magnetic excitation*, because generally

$$(l+1)E_{i_+} = A_{i_+} + \frac{1}{2}lB_{i_+}. \quad (3.23)$$

D. Intersection of  $s$ -channel  $I = \frac{3}{2}$  resonances with the  $t$ -channel pion pole

In pion photoproduction we can also consider the intersection of an  $I_s = \frac{3}{2}$  resonance with the pion pole in the  $t$  channel. Do the zero trajectories killing the double pole at this intersection also have a similar slope in all helicity amplitudes and do they follow the direction  $u = \text{constant}$ ?

The intersection point is now at

$$x_0^* = q_0/|\vec{q}| \approx 1 + \mu^2/(2\vec{q}^2). \quad (3.24)$$

The  $t$ -channel residua of the  $\hat{H}_i$  can be found in Appendix B. Very close to the intersection point, the zero trajectory satisfies

$$u - 2m^2 + M^2 - i\Gamma M = \left(\frac{r^t}{r^s} - 1\right)(s - M^2 + i\Gamma M). \quad (3.25)$$

Defining the zero-trajectory slopes  $\xi_i^\pi$  in the amplitudes  $\hat{H}_i^{(3/2)}$  through

$$\xi_i^\pi = \left. \frac{du}{ds} \right|_{x_0^*} = r_i^t/r_i^s - 1 \quad (3.26)$$

(so that for an Euler- $B$  function with  $\Delta$  and pion poles one would expect  $\xi_i^\pi = 0$ ), instead of Eq. (1.7) we get

$$(1 + \xi_i^\pi) \text{Im}\hat{H}_i^R = -r_i^t/(\Gamma M). \quad (3.27)$$

For the  $\Delta(1232)$  this gives, if we use  $\text{Im}E_{1_+}^{(3/2)R} \approx 0$  and  $\text{Im}M_{1_+}^{(3/2)R} = 0.27 \text{ GeV}^{-1}$

$$\xi_{1;2;3;4}^\pi = -0.98; -0.75; -1.05; -1.02 \quad (3.28)$$

at the intersection point. We see that the zero trajectories follow closely the direction  $t \approx \text{const}$  (which is  $\xi^\pi = -1$ ), i.e., they come *almost parallel* to the pion pole; they are *not* following  $u \approx \text{const}$ .

Since the pion pole in photoproduction is particularly related to the gauge invariance, this *not "hadronlike"* behavior of the pion-pole interaction is very interesting. Any construction of explicit current dual amplitudes should respect this fact. We checked that, going to higher resonances, this situation remains qualitatively the same.

#### IV. COMPTON SCATTERING

We use the Hearn-Leader<sup>22</sup> helicity amplitudes  $\Phi_i (i = 1, \dots, 6)$  but we divide the half-angle factors out. More precisely, we define  $\phi_i$  in terms of the Hearn-Leader  $\Phi_i$  by

$$8\pi W\phi_i = +\Phi_i/\cos(\vartheta/2), \quad \text{for } i = 1, 3, 5 \quad (4.1)$$

$$8\pi W\phi_i = \mp\Phi_i/\sin(\vartheta/2), \quad \text{for } i = 2, 4, 6 \quad (4.2)$$

where  $\vartheta$  is the  $s$ -channel scattering angle, and we shall also use  $x = \cos\vartheta$ . The partial-wave expansion of the  $\phi_i$  reads, if we keep only the terms of parity  $(-1)^{l+1}$ :

$$\phi_{1,2} = \sum_l [(l+2)^2 f_{EE}^{l+1,-} + l^2 f_{MM}^{l+1,-} - 2l(l+2)f_{ME}^{l+1,-}] \times \frac{1}{2}(P_{l+1}^+ \mp P_l^+), \quad (4.3)$$

$$\phi_{3,4} = \pm \sum_l [(l+2)f_{EE}^{l+1,-} - l f_{MM}^{l+1,-} + 2f_{ME}^{l+1,-}] \times \frac{1}{2}(1 \mp x)(P_{l+1}^+ \pm P_l^+), \quad (4.4)$$

$$\phi_{5,6} = \pm \sum_l [f_{EE}^{l+1,-} + f_{MM}^{l+1,-} + 2f_{ME}^{l+1,-}] \frac{1}{2}(1 \pm x)\mathcal{P}_l^+, \quad (4.5)$$

with

$$\mathcal{P}_l^+ \equiv P_{l+1}^+ \mp P_l^+ + (x \mp 1)(P_{l+1}^+ \mp P_l^+). \quad (4.6)$$

The definition of the partial waves  $f_{EE}^{l+1}$ , etc., is as in Contogouris.<sup>23</sup> In the region  $s \leq (m + 2\mu)^2$ , unitarity relates the imaginary parts of the Compton partial waves to single-pion photoproduction multipoles [see Eqs. (C7)–(C9) in Appendix C].

Now we call  $r_i^u$  the residues of the  $u$ -channel nucleon-pole term for the amplitudes  $\phi_i$  with  $I_s = \frac{3}{2}$ . Explicit formulas are listed in Appendix C. For Compton scattering the value of  $x = \cos\vartheta$  at the intersection point of  $s = M^2$  with  $u = m^2$  is

$$x_0 = \frac{M^2 + m^2}{M^2 - m^2}. \quad (4.7)$$

From the six amplitudes  $\phi_i$  we get six equations of the form Eq. (1.7), e.g., from  $\phi_5$  and  $\phi_6$  we obtain

$$(1 + \xi_{5,6}) \text{Im}(f_{EE}^{l+1,-} + f_{MM}^{l+1,-} + 2f_{ME}^{l+1,-}) = \mp \frac{2r_{5,6}^u}{(1 \pm x_0)M_l \Gamma_l \mathcal{P}_l^+(x_0)}. \quad (4.8)$$

##### A. The $\Delta(1232)$ and the $F_{37}(1945)$ resonance

In the  $s$  channel, the  $\Delta(1232)$  can contribute to the Compton partial waves  $f_{EE}^{2-}$ ,  $f_{MM}^{1+}$ , and  $f_{ME}^{1+}$ . Evaluating  $r_i^u$  and the spherical harmonics of argument  $x_0$  for  $s = (1.232)^2$ , we find

$$(1 + \xi_{1,2}) \text{Im}(9f_{EE}^{2-} + f_{MM}^{1+} - 6f_{ME}^{1+}) = \begin{cases} 14.7 \\ 9.5 \end{cases}, \quad (4.9)$$

$$(1 + \xi_{3,4}) \text{Im}(-3f_{EE}^{2-} + f_{MM}^{1+} - 2f_{ME}^{1+}) = \begin{cases} 12.4 \\ 10.2 \end{cases}, \quad (4.10)$$

$$(1 + \xi_{5,6}) \text{Im}(f_{EE}^{2-} + f_{MM}^{1+} + 2f_{ME}^{1+}) = \begin{cases} 6.6 \\ 13.6 \end{cases}. \quad (4.11)$$

Analogously, with  $l=3$  and  $s=(1.945)^2$  we get for the  $F_{37}$  resonance

$$(1 + \xi_{1,2}) \text{Im}(\frac{25}{9}f_{EE}^{4-} + f_{MM}^{3+} - \frac{10}{3}f_{ME}^{3+}) = \begin{cases} 0.27 \\ 0.11 \end{cases}, \quad (4.12)$$

$$(1 + \xi_{3,4}) \text{Im}(-\frac{5}{3}f_{EE}^{4-} + f_{MM}^{3+} - \frac{2}{3}f_{ME}^{3+}) = \begin{cases} 0.17 \\ 0.21 \end{cases}, \quad (4.13)$$

$$(1 + \xi_{5,6}) \text{Im}(f_{EE}^{4-} + f_{MM}^{3+} + 2f_{ME}^{3+}) = \begin{cases} 0.20 \\ 0.19 \end{cases}. \quad (4.14)$$

The numbers on the right-hand side are all taken in units of  $10^{-3} \text{ GeV}^{-1}$ . Of course, all imaginary parts of the partial wave are understood at the respective resonance position. The  $\xi_i$  in Eqs. (4.9)–(4.11) are the zero slopes at the  $\Delta$  intersection, in Eqs. (4.12)–(4.14) at the  $F_{37}$  intersection.

First of all it is remarkable that all values on the right-hand side of Eqs. (4.9)–(4.14) have the same sign as the corresponding  $f_{MM}^{l+}$  term on the left-hand side. Furthermore, the first six numbers center around  $+1.1 \times 10^{-2} \text{ GeV}^{-1}$ , the others around  $+1.9 \times 10^{-4} \text{ GeV}^{-1}$ , so that in both cases a dominant  $f_{MM}^{l+}$  solution is strongly favored. This is, of course, what is expected from photoproduction via the unitarity relation Eq. (C8), since in photoproduction  $M_{1+}^{3/2}$  ( $M_{3+}^{3/2}$ ) strongly dominate over  $E_{1+}^{3/2}$  ( $E_{3+}^{3/2}$ ).

What about the predicted size of the resonant multipoles? Phenomenological analyses of Compton scattering in the  $\Delta(1232)$  energy range give<sup>24</sup>

$$\text{Im}f_{MM}^{1+ (3/2)} (W=M_\Delta) = 1.7 \times 10^{-2} \text{ GeV}^{-1}, \quad (4.15)$$

and  $f_{EE}^{2-}$  and  $f_{ME}^{1+}$  small, so that the  $\xi_i$  have to be slightly negative, but not large. For the  $F_{37}$ , using the multiple-analysis value Eq. (3.12) we get

$$\text{Im}f_{MM}^{3+R} \geq 1.0 \times 10^{-4} \text{ GeV}^{-1}. \quad (4.16)$$

This is consistent with Eqs. (4.12)–(4.14) for small  $\xi_i$  if we neglect  $f_{EE}^{4-}$  and  $f_{ME}^{3+}$  and take into account that the  $F_{37}(1945)$  is only to  $\sim 40\%$  coupled to the elastic  $\pi$ - $N$  channel.

#### B. High-energy limit

The residues  $r_i^u$  simplify for  $s \gg m^2$  (see Appendix C). The angular terms of the partial-wave expansion Eqs. (4.3)–(4.5) are again approximated by modified Bessel functions since

$$x_0 \approx -1 - 2m^2/s \quad (4.17)$$

gets close to  $-1$ . Apart from Eqs. (2.14), (2.15),

(3.14), and (3.15), we use for Eq. (4.6)

$$\mathcal{O}_i^+(x_0) \approx (-1)^{l+1} [2l(l+1)(l+2)]^2 I_3(R)/R^3, \quad (4.18)$$

$$\mathcal{O}_i^-(x_0) \approx (-1)^{l+1/2} l(l+1)(l+2) I_0(R), \quad (4.19)$$

with  $R$ , as usual, given by Eq. (2.16). With these approximations, the equations of type (4.8) become, if we consider peripheral resonances, Eq. (2.19):

$$(1 + \xi_{1,2}) b^{-1} \text{Im}(f_{EE}^{l+1,-} + f_{MM}^{l+} - 2f_{ME}^{l+}) = (\kappa \pm 1)^2 / I_{1,0}(R), \quad (4.20)$$

$$(1 + \xi_{3,4}) b^{-1} \text{Im}(-f_{EE}^{l+1,-} + f_{MM}^{l+}) = \frac{\kappa^2 - 1}{I_{1,2}(R)}, \quad (4.21)$$

$$(1 + \xi_{5,6}) b^{-1} \text{Im}(f_{EE}^{l+1,-} + f_{MM}^{l+} + 2f_{ME}^{l+}) = \frac{(\kappa \mp 1)^2}{I_{3,0}(R)}, \quad (4.22)$$

with

$$b = \frac{2R}{137a^4 W^4 \Gamma}. \quad (4.23)$$

For  $R=5$ , the numbers appearing in the right-hand side of Eqs. (4.20)–(4.22) are, 1.34, 0.50, 0.87, 1.21, 1.33, and 1.20, respectively. Although there is some spread in these numbers, it is again remarkable that they are all positive and close to each other. An approximate solution may take all  $\xi_i$  equal and neglect the  $f_{EE}^{l+1,-}$ ,  $f_{ME}^{l+}$ , leading to

$$\text{Im}f_{MM}^{l+R} \approx \frac{1.1b}{1 + \xi}. \quad (4.24)$$

What is the contribution of these resonances to the total cross section? If we keep only the partial waves  $f_{MM}^{l+}$ ,

$$\sigma_{\text{tot}} = \frac{4\pi W}{s - m^2} \sum l^2 (l+1) \text{Im}f_{MM}^{l+}. \quad (4.25)$$

In the narrow-resonance approximation, Eq. (4.24) leads to

$$\text{Im}f_{MM}^{l+} \approx \frac{1.1b\Gamma_l M_l}{1 + \xi_l} \pi \delta(s - M_l^2), \quad (4.26)$$

or, since we consider only peripheral resonances and take  $s \gg m^2$ ,

$$\sigma_{\text{tot}}^{(3/2)} \approx \sum_l \frac{1.1\pi^2 \delta(s - M_l^2)}{137aM_l(1 + \xi_l)} \approx \frac{15 \mu\text{b GeV}^{-1}}{s(1 + \xi)}. \quad (4.27)$$

This is a reasonable order of magnitude, even if  $\xi$  is neglected. Of course, like in Eq. (2.27) one rather expects a behavior as  $s^{-1/2}$ , so that nonperipheral resonances or an energy dependence of  $\xi$  must be present.

#### V. PION PRODUCTION BY AN AXIAL-VECTOR CURRENT

The last process which we shall consider is axial-vector-current pion production. Just as in

photoproduction, we use helicity amplitudes, here called  $\hat{K}_i$ , which have the half-angle factors removed. In contrast to Sec. III, however, here we shall adhere to Adler's normalization conventions.<sup>25</sup> Equations (D1)–(D3) in Appendix D give the relation of our  $\hat{K}_i$  to Adler's  $g_i^A$ . In Appendix D we also list the partial-wave expansions of the  $\hat{K}_i$  in terms of axial-vector multipole amplitudes  $\mathfrak{M}_{i+}$ ,  $\mathcal{E}_{i+}$ ,  $\mathcal{L}_{i+}$ , etc.,  $k_0$  and  $|\vec{k}|$  denote the c.m. energy and three-momentum of the current. We shall also use

$$\lambda^2 = \vec{k}^2 - k_0^2. \quad (5.1)$$

#### A. The $\Delta(1232)$ resonance for $\lambda^2 = 0$

We consider first the intersection of the  $\Delta(1232)$  with  $u = m^2$ . We restrict ourselves to  $\lambda^2 = 0$  and  $I_s = \frac{3}{2}$ . Denoting the zero-trajectory slopes in the amplitudes  $\hat{K}_i$  for  $I_s = \frac{3}{2}$  by  $\xi_i$ , we get

$$(1 + \xi_{1,3}) \text{Im}(\mathfrak{M}_{1+}^R + \mathcal{E}_{1+}^R) = \begin{cases} -36.6 \\ -37.8 \end{cases}, \quad (5.2)$$

$$(1 + \xi_{2,4}) \text{Im}(3\mathfrak{M}_{1+}^R - \mathcal{E}_{1+}^R) = \begin{cases} +32.6 \\ +39.5 \end{cases}, \quad (5.3)$$

$$(1 + \xi_{5,6}) \text{Im}\mathcal{L}_{1+}^R = \begin{cases} +21.3 \\ +19.6 \end{cases}, \quad (5.4)$$

where our unit is  $\text{GeV}^{-1}$ .

We see that the slopes come out to be pairwise equal. Demanding also  $\xi_1 \approx \xi_2$  or  $\xi_3 \approx \xi_4$  we get  $\text{Im}\mathfrak{M}_{1+}^R \ll \text{Im}\mathcal{E}_{1+}^R$ . From  $\xi_1 \approx \xi_5$  or  $\xi_3 \approx \xi_6$  we get  $\text{Im}\mathcal{E}_{1+}^R \approx -2 \text{Im}\mathcal{L}_{1+}^R$ . Comparing this to Adler's values,<sup>25</sup>

$$\text{Im}\mathcal{E}_{1+}^R = -\frac{8\pi m g_A}{g\bar{q}^2} = -42 \text{ GeV}^{-1}, \quad (5.5)$$

$$\text{Im}\mathfrak{M}_{1+}^R \ll \text{Im}\mathcal{E}_{1+}^R, \quad (5.6)$$

$$-2\mathcal{L}_{1+} = \mathcal{E}_{1+}, \quad (5.7)$$

we see an excellent agreement. Comparing Eq. (5.2) with (5.5), even the numerical value of  $\mathcal{E}_{1+}^R$  comes out correctly if the  $\xi_i$  are small.

#### B. Higher resonances for $\lambda^2 = 0$

Unfortunately the success of our argument this time does not continue (which, by the way, shows that the agreement obtained in the former cases was not trivial). If we consider the  $F_{37}(1945)$ -nucleon-pole intersection, always for  $\lambda^2 = 0$ , we find (unit is again  $\text{GeV}^{-1}$ )

$$(1 + \xi_{1,3}) \text{Im}(\mathfrak{M}_{3+}^R + \mathcal{E}_{3+}^R) = \begin{cases} -0.73 \\ -1.36 \end{cases}, \quad (5.8)$$

$$(1 + \xi_{2,4}) \text{Im}(5\mathfrak{M}_{3+}^R - 3\mathcal{E}_{3+}^R) = \begin{cases} +1.77 \\ +4.15 \end{cases}, \quad (5.9)$$

$$(1 + \xi_{5,6}) \text{Im}\mathcal{L}_{3+}^R = \begin{cases} +0.92 \\ +0.82 \end{cases}. \quad (5.10)$$

Whereas  $\xi_5 \approx \xi_6$  is still satisfied, we see that  $\xi_1 \approx \xi_3$  and  $\xi_2 \approx \xi_4$  are no longer true. This becomes more pronounced if we consider the high- $s$  limit, using the same approximations as in Secs. II–IV. Appendix D contains the high-energy expressions for the  $r_i^u$ . For peripheral resonances according to Eqs. (2.19) and (2.20) we get for  $s \gg m^2, l \gg 1$ ,

$$(1 + \xi_{1,3}) \text{Im}(\mathfrak{M}_{1+}^R + \mathcal{E}_{1+}^R) = \begin{cases} -\frac{md_1}{WI_2(R)} \\ -\frac{Wd_1}{2mI_1(R)} \end{cases}, \quad (5.11)$$

$$(1 + \xi_{2,4}) \text{Im}(\mathfrak{M}_{1+}^R - \mathcal{E}_{1+}^R) = \begin{cases} +\frac{md_1}{WI_1(R)} \\ +\frac{Wd_1}{2mI_0(R)} \end{cases}, \quad (5.12)$$

$$(1 + \xi_{5,6}) \text{Im}\mathcal{L}_{1+}^R = \begin{cases} +d_1/I_1(R) \\ +\frac{1}{2}d_1/I_0(R) \end{cases}, \quad (5.13)$$

where we have used the abbreviation

$$d_1 = 16mg_{AG}/(W^3 a^2 \Gamma). \quad (5.14)$$

We can still have  $\xi_1 \approx \xi_2$  and  $\xi_3 \approx \xi_4$  so that  $\mathfrak{M}_{1+} \ll \mathcal{E}_{1+}$ . However, the pair of equations (5.11) [and also the pair of Eqs. (5.12)] contain different energy dependences on the right-hand side. So a solution with  $\xi_1 \approx \xi_3$  and  $\xi_2 \approx \xi_4$  is not possible. This is in contrast to the three reactions treated in Secs. II–IV, where the energy dependences in Eqs. (2.18), (3.16) and (3.17), (4.20)–(4.22) all matched, so that we could have equal slopes  $\xi_i$ . Why the case of axial-vector-current pion production does not have this property remains an open question.

## VI. $I = \frac{1}{2}$ RESONANCES AND ISOSPIN PROBLEMS

In Secs. II–V we considered only  $I = \frac{3}{2}$  resonances in the  $s$  channel. Unfortunately, the same procedure cannot be expected to be successful in the case of  $s$ -channel  $I = \frac{1}{2}$  resonances, i.e., the helicity structure of the excitation of  $I = \frac{1}{2}$  resonances cannot be obtained by simply assuming equal zero-trajectory slopes in all helicity amplitudes at the intersection with the  $u$ -channel nucleon pole. Already a glance at the phenomenologically determined zeros of photoproduction amplitudes

in Ref. 10 shows that for  $I_s = \frac{1}{2}$  the zero trajectories behave very differently in different spin amplitudes. This is not surprising.

Generally in a dual model the complete amplitude is a superposition of  $s/t$ ,  $s/u$ , and  $t/u$  dual terms. Assume that each single dual term has the same simple zero structure for all helicities (e.g., like that of a Veneziano Euler- $B$  function). Now it can happen that a certain pole appears in more than one dual term, e.g., an  $s$ -channel resonance can appear in the  $s/t$  and  $s/u$  terms. Then the residue of the resonance is split up in two parts and the total residue does not reflect the simple zero structure of the single-dual terms. Observe that we are studying only ratios of *pole residues*. So the mere presence of more than one dual term does not disturb the zero slopes at the pole intersections, as long as a pole does not appear in more than one term.

We believe that our success of revealing a simple structure in the  $I_s = \frac{3}{2}$  amplitude reflects the fact that probably the whole series of  $\Delta$  resonances and the dominant part of the  $u$ -channel nucleon pole is contained in one single-dual term. However, for the  $I_s = \frac{1}{2}$  resonances one has to face seriously the problem of how to split up the residues in order to achieve a simple structure of each term. We think that this splitting might be solved by using a purely algebraic procedure.

The particular choice of isospin amplitudes is irrelevant, as long as we only require different helicity amplitudes to have the same zero-trajectory slopes  $\xi_i$ . However, the actual magnitude of the  $\xi_i$  (remember that in many cases we obtained good absolute predictions for the resonance couplings by assuming that the  $\xi_i$  are small) depends on the choice of the isospin amplitudes made. For example, instead of projecting the nucleon pole on  $I_s = \frac{3}{2}$ , we may have projected the  $\Delta$  on  $I_u = \frac{1}{2}$ . Fortunately, for the combination of  $I_s = \frac{3}{2}$  resonances, with an  $I_u = \frac{1}{2}$  pole term, various simple choices of the basic isospin amplitudes lead to numerically very similar results for the ratios of the pole residues, and so also for the  $\xi_i$ . We show this in the following.

If

$$A^{(3/2)} = \frac{r_s}{s - M^2} + \frac{r_u}{u - m^2}, \quad (6.1)$$

then the *ratios* of the residua in the standard<sup>26</sup> crossing-even and -odd ( $\pm$ ) amplitudes following from Eq. (6.1),

$$A^{(\pm)} = \frac{1}{6} \left( \frac{4r_s}{s - M^2} + \frac{3r_u}{u - m^2} \right) \quad (6.2)$$

and

$$A^{(-)} = -\frac{1}{6} \left( \frac{2r_s}{s - M^2} + \frac{3r_u}{u - m^2} \right) \quad (6.3)$$

differ only by a factor  $\frac{4}{3}$  or  $\frac{2}{3}$ , respectively. If we used the amplitude with  $I_u = \frac{1}{2}$ , Eq. (6.1) would become

$$A^{(u, 1/2)} = \frac{1}{6} \left( \frac{8r_s}{s - M^2} + \frac{9r_u}{u - m^2} \right), \quad (6.4)$$

so that the residue ratio gets a factor  $\frac{8}{9}$ . So, if we choose the "wrong" isospin basis, the numbers for the ratios of the residues come out differently only by 15 ··· 40%. The order of magnitude and the signs are all the same for the four cases Eqs. (6.1)–(6.4).

The situation is quite different if we consider the intersection of an  $I_s = \frac{1}{2}$  resonance with the  $u$ -channel nucleon pole. In this case, if

$$A^{(1/2)} = \frac{r_s}{s - M^2} + \frac{r_u}{u - m^2}, \quad (6.5)$$

this becomes, in terms of  $A^{(\pm)}$ ,

$$A^{(\pm)} = \frac{r_s}{s - M^2} \mp \frac{3r_u}{u - m^2}, \quad (6.6)$$

or, for the  $I_u = \frac{1}{2}$  isospin amplitude,

$$A^{(u, 1/2)} = \frac{r_s}{s - M^2} - \frac{9r_u}{u - m^2}. \quad (6.7)$$

We see that here signs and numbers differ drastically. So, unless one can put forward a criterion for which isospin amplitude should be used, with  $I_s = \frac{1}{2}$  resonances it does not make sense to expect, e.g.,  $r_s \approx r_u$  or  $\xi_i \approx 0$ .

## VII. CONCLUSIONS

Quite generally, if an amplitude has poles in different channels (e.g., resonances in the  $s$  and  $u$  channel), it also has zero trajectories (i.e., manifolds where the amplitude is zero) in the complex Mandelstam "plane" which pass through the intersections of the poles. In this paper we considered the slopes  $\xi$  of these zero trajectories in the Mandelstam plane for the case of reactions involving particles with spin or currents. Since we always assumed narrow resonances, we could study the slopes in the real  $s$ - $t$  plane. We studied the possibility of whether at particular intersections of poles the zero-trajectory slopes  $\xi_i$  in all helicity amplitudes  $f_i$  of the same process may be equal.

The interest in this feature comes from dual models. For example, Veneziano Euler- $B$ -function models prescribe specific slopes  $\xi_i$ . However, dual models have met serious problems when one tried to apply them to the phenomenology of reactions involving fermions or currents.

So, if at least our "equal zero-trajectory slope" hypothesis is verified, this would show one good "dual" property of fermion or current amplitudes.

We concentrated on the intersections of  $I=\frac{3}{2}$  resonances in the  $s$  channel with the  $u$ -channel nucleon pole and studied these for several processes (the case of  $I=\frac{1}{2}$  resonances is expected to be more complicated). It turns out that our hypothesis is quite powerful and leads to a number of nontrivial predictions which are in agreement with the data. The more complicated the spin structure of the process considered is (e.g., nucleon Compton scattering), the more remarkable is the consistency of the equations which follow from the "equal zero-trajectory slope" hypothesis.

In particular, we get the following:

(1) In pion-nucleon scattering  $I=\frac{3}{2}$  resonances can be dominant only if they have odd  $l$ . For  $\Delta$ -type resonances [i.e.,  $l$  odd, parity  $(-1)^{l+1}$ ] the zero-trajectory slopes at the intersection with the nucleon pole *come out* to be accurately equal in both helicity amplitudes already *without* our hypothesis.

(2) We treat the high-energy case explicitly using a modified Bessel-function approximation. We get a formula expressing the nondiffractive  $\pi^*p$  cross section in terms of the zero-trajectory slopes  $\xi$ .

(3) In pion photoproduction and Compton scattering the  $\Delta$ -type resonances must be excited dominantly by magnetic multipoles (in agreement with quark-model predictions).

(4) Making the assumption that the zero-trajectory slopes behave at least qualitatively as in an Euler- $B$ -function model, we can also exclude dominant  $\pi$ - $N$  resonances with  $I=\frac{3}{2}$  and parity  $(-1)^l$  (in agreement with the data).

(5) If we now assume very specifically that the zero trajectories follow approximately the direction  $t = \text{constant}$  at the  $s$ -channel- $\Delta$ - $u$ -channel-nucleon pole intersection, we can predict the absolute values of the  $\Delta$  and  $F_{37}$  couplings, i.e., the  $\Delta$  width, the  $F_{37}$  elasticity, and the photoproduction amplitudes  $M_{1+}^{(3/2)}$  and  $M_{3+}^{(3/2)}$ . In our narrow-resonance approximation these agree within 30% with the phenomenological data. With the same assumption the formula referred to above in (2) gives the correct order of magnitude of the nondiffractive  $\pi^*p$  cross section.

(6) For axial-vector-current  $\Delta(1232)$  excitation we get results very similar to those of Adler.<sup>25</sup> However, for higher-resonance production by the axial-vector current we encounter difficulties.

#### ACKNOWLEDGMENTS

We thank V. Rittenberg for useful discussions during the course of our work. We are particularly

grateful to R. Wilcke, whose phenomenological study of photoproduction-amplitude zeros stimulated this investigation. Thanks are also due to G. Höhler and I. Sabba Stefanescu for discussions about zero trajectories.

#### APPENDIX A

Here we list some definitions and properties of pion-nucleon elastic scattering amplitudes which we use in Sec. II.

In terms of the standard center-of-mass spin amplitudes  $f_1, f_2$  (see e.g., Ref. 26):

$$d\sigma/d\Omega = \sum |\langle f | f_1 + (\vec{\sigma} \cdot \hat{q}') (\vec{\sigma} \cdot \hat{q}) f_2 | i \rangle|^2, \quad (\text{A1})$$

where  $\hat{q}$  and  $\hat{q}'$  denote c.m. unit vectors along the directions of the incoming and outgoing pion, respectively; we define our  $f_{\pm}$  by

$$f_{\pm} = f_1 \pm f_2. \quad (\text{A2})$$

The partial-wave expansion of the  $f_{\pm}$  has the form

$$f_{\pm} = \sum_l [f_{l\pm} \pm f_{l\pm, -}] [P'_{l\pm}(x) \mp P_l(x)], \quad (\text{A3})$$

with  $x = (\hat{q} \cdot \hat{q}')$ , the cosine of the c.m. scattering angle  $\vartheta$ .

For  $I_s = \frac{3}{2}$ , the  $u$ -channel nucleon-pole contributions to the  $f_{\pm}$  are

$$f_{\pm} = r_{\pm}^u / (u - m^2) + \dots, \quad (\text{A4})$$

where  $(g^2/4\pi = 14.6)$

$$r_{\pm}^u = \frac{g^2}{2\pi W} (Wq_0 - \mu^2), \quad r_{\pm}^u = \frac{g^2}{2\pi W} mq_0. \quad (\text{A5})$$

$W$  and  $q_0$  are the total and pion c.m. energies,  $|\vec{q}|$  is the c.m. pion momentum.  $m$  and  $\mu$  denote the nucleon and pion masses, respectively. At the intersection of the nucleon pole  $u = m^2$  with a resonance pole at  $s = M^2$ ,  $x$  has the unphysical value  $x_0$ :

$$x_0 = (-Eq_0 + \mu^2/2) / \vec{q}^2, \quad (\text{A6})$$

where  $q_0$ ,  $\vec{q}^2$ , and  $E = W - q_0$  have to be evaluated for  $s = M^2$ .

#### APPENDIX B

In our treatment of single-pion photoproduction in Sec. III we used several definitions and formulas for the pole-term residues, which we list in the following.

Our amplitudes  $\hat{H}_i$  are related to the standard c.m. spin amplitudes  $\mathcal{F}_1, \dots, \mathcal{F}_4$  of Chew *et al.*<sup>27</sup> by

$$\hat{H}_{1,3} = \mp \mathcal{F}_3 - \mathcal{F}_4, \quad (\text{B1})$$

$$\hat{H}_{2,4} = \mp \mathcal{F}_1 + \mathcal{F}_2 + (1 \mp x)(\mathcal{F}_3 \mp \mathcal{F}_4)/2. \quad (\text{B2})$$

The corresponding  $u$ -channel nucleon-pole and  $t$ -channel pole contributions, projected to  $I_s = \frac{3}{2}$ , are written as

$$\hat{H}_i^{3/2} = r_i^u / (u - m^2) + r_i^t / (t - \mu^2) + \dots, \quad (\text{B3})$$

where the nucleon-pole residues  $r_i^u$  are explicitly given by

$$r_{1,3}^u = -\gamma |\vec{q}| \left[ \left( \frac{(W^2 - m^2)g_V}{2m} - m \right) (1 \pm v) - W(1 \mp v) \right], \quad (\text{B4})$$

$$r_{2,4}^u = -\frac{1}{2}\gamma \left[ \left( \frac{(W^2 - m^2)g_V}{2} + \mu^2 - m^2 \right) (1 \pm v) - Wm(1 \mp v) \right], \quad (\text{B5})$$

with

$$\gamma = \beta [(W - m)^2 - \mu^2]^{1/2} / s, \quad (\text{B6})$$

$$v = \{ [(W + m)^2 - \mu^2] / [(W - m)^2 - \mu^2] \}^{1/2}, \quad (\text{B7})$$

and  $g_V = 3.706$ ,  $\beta = eg/8\pi = 0.163$ . The pion-pole residues are

$$r_{1,3}^t = \gamma |\vec{q}| [W + m \mp v(W - m)], \quad (\text{B8})$$

$$r_{2,4}^t = -\gamma \mu^2 (1 \pm v) / 2. \quad (\text{B9})$$

For  $s \gg \mu^2$  this simplifies to

$$r_{1,2}^u = -\beta |\vec{q}| g_V (2 |\vec{q}| / m; 1), \quad (\text{B10})$$

$$r_{3,4}^u = \beta m |\vec{q}| (g_V + 2) (2 |\vec{q}| / m; 1) / W, \quad (\text{B11})$$

$$r_1^t = -r_4^t = -\beta m \mu^2 / s, \quad (\text{B12})$$

$$r_{2,3}^t = \beta (-\mu^2; 4\vec{q}^2) / W. \quad (\text{B13})$$

#### APPENDIX C

Here we collect some formulas which we used in our treatment of Compton scattering in Sec. IV.

The residues  $r_i^u$  of the  $u$ -channel nucleon-pole terms are defined through

$$\phi_i^{(3/2)} = r_i^u / (u - m^2) + \dots, \quad (\text{C1})$$

where the  $\phi_i$  are defined in Eqs. (4.1) and (4.2).

Using the paper of Fox and Freedman,<sup>28</sup> in particular their Eqs. (7), (A2), and Table I, one obtains

$$r_{1,5}^u = f[-4m^2 + (s - m^2)(\kappa \pm 1)^2], \quad (\text{C2})$$

$$r_{2,6}^u = \frac{m}{W} f[4m^2 + (s - m^2)(\kappa \mp 1)^2], \quad (\text{C3})$$

$$r_3^u = f[4m^2 + (s - m^2)(\kappa^2 - 1)], \quad (\text{C4})$$

$$r_4^u = \frac{m}{W} f[-4m^2 + (s - m^2)(\kappa^2 - 1)], \quad (\text{C5})$$

where

$$f = \frac{1}{137(8W)}, \quad (\text{C6})$$

and  $\kappa$  is defined in Eq. (3.17). In the high-energy limit  $s \gg m^2$  one simply drops all  $m^2$  in Eqs. (C2)–(C5).

Unitarity tells us for  $s \leq (m + 2\mu)^2$ ,

$$\text{Im} f_{EE}^{I^*+1, -} = |\vec{q}| |E_{I^*}|^2, \quad (\text{C7})$$

$$\text{Im} f_{MM}^{I^*} = |\vec{q}| |M_{I^*}|^2, \quad (\text{C8})$$

$$\text{Im} f_{ME}^{I^*} = -|\vec{q}| \text{Re}(E_{I^*} M_{I^*}^*), \quad (\text{C9})$$

where the multipole amplitudes of photoproduction on the right-hand side are normalized as in CGLN,<sup>27</sup> and on both sides isospin  $I_s = \frac{3}{2}$  amplitudes are understood.  $|\vec{q}|$  is the pion c.m. momentum. For  $s > (m + 2\mu)^2$  these equations provide only lower bounds for the imaginary parts of the Compton partial waves.

#### APPENDIX D

Here we give the formulas relevant for our calculation of axial-vector-current pion production in Sec. V. Our helicity amplitudes  $\hat{K}_i$  are defined in terms of Adler's  $\mathcal{G}_i^A$  by

$$\hat{K}_{1,3} = -\mathcal{G}_3^A \mp \mathcal{G}_4^A, \quad (\text{D1})$$

$$\hat{K}_{2,4} = \mathcal{G}_1^A \mp \mathcal{G}_2^A + \frac{1}{2}(1 \mp x)(\mathcal{G}_4^A \mp \mathcal{G}_5^A), \quad (\text{D2})$$

$$\hat{K}_{5,6} = \mathcal{G}_5^A \pm \mathcal{G}_6^A. \quad (\text{D3})$$

Observe that in Sec. V we consequently use amplitudes normalized according to Adler's conventions. Defining partial-wave amplitudes in terms of Adler's  $\mathfrak{M}_l, \mathcal{E}_l$ , etc. by

$$\mathfrak{A}_{I^*} = \frac{1}{2}[(l+2)\mathfrak{M}_{I^*} - l\mathcal{E}_{I^*}], \quad (\text{D4})$$

$$\mathfrak{B}_{I^*} = -\mathfrak{M}_{I^*} - \mathcal{E}_{I^*}, \quad (\text{D5})$$

$$\mathfrak{C}_{I^*} = -k_0(l+1)\mathcal{E}_{I^*} / |\vec{k}| \quad (\text{D6})$$

(we shall not use the corresponding  $\hat{\mathfrak{A}}_{I^*}$ , etc.), the partial-wave expansions of the  $\hat{K}_i$  take the same form as Eqs. (3.1) and (3.2):

$$\hat{K}_{1,3} = \sum_l (\mathfrak{A}_{I^*} \mp \mathfrak{B}_{I^*}) (P_l' \mp P_{l+1}'), \quad (\text{D7})$$

$$\hat{K}_{2,4} = \sum_l (\mathfrak{A}_{I^*} \mp \mathfrak{B}_{I^*}) (P_l' \mp P_{l+1}'), \quad (\text{D8})$$

$$\hat{K}_{5,6} = \sum_l (\mathfrak{C}_{I^*} \mp \mathfrak{C}_{I^*}) (P_l' \mp P_{l+1}'). \quad (\text{D9})$$

The  $u$ -channel nucleon-pole residues  $r_i^u$  of our amplitudes  $\hat{K}_i$  with  $I_s = \frac{3}{2}$  are easily obtained from the nucleon-pole terms of the  $\mathcal{G}_i^A$ , using Eqs. (D1)–(D3). The crossed-nucleon-pole terms of the  $\mathcal{G}_i^A$  for  $I_s = \frac{3}{2}$  are

$$\mathcal{G}_{1,2}^{Au} = \pm \frac{|\vec{q}| (W \pm m) \mathcal{O}_{1\pm}}{2m(W - q_0 \pm m)} A_{1\pm}^u, \quad (\text{D10})$$

$$g_{3,4}^{A_u} = \pm \frac{|\vec{q}| \mathcal{O}_{1\mp}}{m} A_1^u, \quad (\text{D11})$$

$$g_{5,6}^{A_u} = \frac{\mathcal{O}_{1\mp}}{2m\vec{k}^2} [2mk_0(W \pm m) \pm \lambda^2(W \pm m - 2q_0)] A_1^u, \quad (\text{D12})$$

where

$$\mathcal{O}_{1\pm} = [(W - k_0 \pm m)(W - q_0 \pm m)]^{1/2} \quad (\text{D13})$$

and

$$A_1^u = \frac{2g_A g}{u - m^2}. \quad (\text{D14})$$

$g$  has been given in Appendix A,  $g_A = 1.26$ . In the limit  $s \gg \mu^2$ , the residues  $r_i^u$  of the  $\hat{K}_i^{I=3/2}$  take a quite simple form:

$$\begin{aligned} r_1^u &= 4 |\vec{q}| g_A g, & r_2^u &= -2mg_A g, \\ r_3^u &= -\frac{W^4 - m^4}{W^2 m} g_A g, & r_4^u &= \frac{W^2 + m^2}{W} g_A g, \\ r_5^u &= 4Wg_A g, & r_6^u &= -4mg_A g. \end{aligned} \quad (\text{D15})$$

- <sup>1</sup>G. Veneziano, *Nuovo Cimento* **57A**, 190 (1968); for a comprehensive review, see, e.g., Ref. 8.
- <sup>2</sup>C. Lovelace, *Phys. Lett.* **28B**, 264 (1968).
- <sup>3</sup>G. Altarelli and H. R. Rubinstein, *Phys. Rev.* **183**, 1469 (1969).
- <sup>4</sup>B. Peterson and N. A. Törnqvist, *Nucl. Phys.* **B13**, 629 (1969).
- <sup>5</sup>C. DeTar, K. Kang, C. I. Tam, and J. H. Weis, *Phys. Rev. D* **4**, 425 (1971).
- <sup>6</sup>E. L. Berger and G. C. Fox, *Phys. Rev.* **188**, 2120 (1969).
- <sup>7</sup>E. N. Argyres, A. P. Contogouris, C. S. Lam, and S. Ray, *Nuovo Cimento* **4A**, 156 (1971); M. Ahmad, Fayyazudin, and Riazuddin, *Phys. Rev. Lett.* **23**, 504 (1969).
- <sup>8</sup>M. Fukugita and K. Igi, *Phys. Rep.* **31C**, 237 (1977); P. H. Frampton, *Dual Resonance Models* (Benjamin, New York, 1974).
- <sup>9</sup>R. Odorico, *Nucl. Phys.* **B37**, 509 (1972); *Phys. Rev. D* **8**, 3952 (1973).
- <sup>10</sup>G. v. Gehlen, W. Pfeil, and R. Wilcke, report, Bonn University (unpublished); R. Wilcke, Diploma thesis, Bonn University Report No. BONN-IR-76-3, 1976 (unpublished).
- <sup>11</sup>W. J. Metcalf and R. L. Walker, *Nucl. Phys.* **B76**, 253 (1974); R. G. Moorhouse, H. Oberlack, and A. H. Rosenfeld, *Phys. Rev. D* **9**, 1 (1974); I. M. Barbour, R. L. Crawford, and N. H. Parsons, *Nucl. Phys.* **B141**, 253 (1978).
- <sup>12</sup>E. Borie, W. Gampp, G. Höhler, R. Koch, and I. Sabba Stefanescu, University of Karlsruhe Report No. TKP-78-18, 1978 (unpublished); G. Höhler and I. Sabba Stefanescu, *Z. Phys. C* **1**, 253 (1979).
- <sup>13</sup>D. M. Chew and M. Urban, in *Proceedings of the Topical Conference on Baryon Resonances, Oxford 1976* (Rutherford Laboratory, Chilton, 1976), p. 156; D. M. Chew, *Phys. Rev. D* **18**, 2368 (1978).
- <sup>14</sup>For example, T. Eguchi, T. Shimada, and M. Fukugita, *Nucl. Phys.* **B74**, 102 (1974).

- <sup>15</sup>G. F. Chew and F. E. Low, *Phys. Rev.* **101**, 1570 (1956).
- <sup>16</sup>Particle Data Group, *Phys. Lett.* **75B**, 1 (1978).
- <sup>17</sup>L. Durand III and Y. T. Chiu, *Phys. Rev.* **139**, B646 (1965).
- <sup>18</sup>B. Schrempp and F. Schrempp, *Nucl. Phys.* **B54**, 525 (1973).
- <sup>19</sup>G. Höhler and H. P. Jakob, Karlsruhe University Report No. TKP-23/72, 1972 (unpublished).
- <sup>20</sup>R. L. Walker, *Phys. Rev.* **182**, 1729 (1969).
- <sup>21</sup>Using the c.m. spin amplitudes  $\mathcal{F}_i$  of Chew *et al.*<sup>27</sup> and calling the zero-trajectory slopes in these amplitudes  $\xi_i$ , we get a quite remarkable pattern (we neglect  $E_{1\pm}^R$ , our unit is  $\text{GeV}^{-1}$ ):
- $$\begin{aligned} -12.72(1 + \xi_1)\text{Im}M_{1\pm}^R &= -2.47, \\ +2(1 + \xi_2)\text{Im}M_{1\pm}^R &= +0.30, \\ -3(1 + \xi_3)\text{Im}M_{1\pm}^R &= -0.58, \\ 0(1 + \xi_4)\text{Im}M_{1\pm}^R &= +0.04. \end{aligned}$$

The numerical values of the Legendre polynomials at  $x_0$  [ $P_2'(x_0) = -12.72, \dots, P_1'' = 0$ ] follow very closely the pattern of the nucleon-pole residues ( $-2.47, \dots, +0.04$ ).  $\mathcal{F}_4$  contains no  $\Delta$  pole to which it corresponds that its nucleon-pole residue happens to vanish near  $s = M_\Delta^2$ .

- <sup>22</sup>A. C. Hearn and E. Leader, *Phys. Rev.* **126**, 789 (1962).
- <sup>23</sup>A. P. Contogouris, *Nuovo Cimento* **25**, 104 (1962).
- <sup>24</sup>W. Pfeil, H. Rollnik, and S. Stankowski *Nucl. Phys.* **B73**, 166 (1974).
- <sup>25</sup>S. Adler, *Ann. Phys. (N.Y.)* **50**, 189 (1968).
- <sup>26</sup>G. F. Chew, M. L. Goldberger, F. Low, and Y. Nambu, *Phys. Rev.* **106**, 1337 (1957).
- <sup>27</sup>G. F. Chew, M. L. Goldberger, F. E. Low, and Y. Nambu, *Phys. Rev.* **106**, 1345 (1957).
- <sup>28</sup>G. C. Fox and D. Z. Freedman, *Phys. Rev.* **182**, 1628 (1969).